GMR
The Original

ANTICANCER POTENTIAL OF SUSTAINABLE MULTISCALE POLYMERIC (STARCH/PVA/CUO) ELECTROSPUN NANOSCAFFOLDS FROM *POCOCKIELLA VARIEGATA* (BROWN MARINE MACROALGAE) EXTRACT

Srinidhi Rajaraman[1], Akilesh Anbalagan[2], Priya Ramji[3], Balaguru Natarajan[4], Alagendran Subbarayalu[5], Kaliyamoorthy Dass[6*]

[1]Saveetha Medical College & Hospital (SMCH), Saveetha Institute of Medical and Technical Sciences (SIMATS), Thandalam, Chennai, Tamil Nadu 602105, India. Email: srinidhirajaraman04@gmail.com
[2]Department of Anaesthesia, Saveetha Medical College and Hospital, Saveetha Institute of Medical And Technical Sciences (SIMATS), Thandalam, Chennai-602105, Tamil Nadu, India. Email: dr.akilesh97@gmail.com; ORCID: https://orcid.org/0009-0008-3742-6538
[3]Department of Bioinformatics, School of Life Sciences, Vels Institute of Science Technology and Advanced Studies, Pallavaram, Chennai-600117, Tamil Nadu, India. Email: priya.microbio@gmail.com; ORCID: https://orcid.org/0000-0002-9244-6194
[4]Department of Dermatology, Saveetha Medical College and Hospital, Saveetha Institute of Medical And Technical Sciences (SIMATS), Thandalam, Chennai-602105, Tamil Nadu, India. Email: bala1guru@gmail.com; ORCID: https://orcid.org/0009-0007-4000-0469
[5]Saveetha College of Nursing (SCON), Saveetha Institute of Medical and Technical Sciences (SIMATS), Chennai – 602105, Tamil Nadu, India. Email: alagendrans.scon@saveetha.com; ORCID: https://orcid.org/0009-0009-0749-7180
[6]Natural Product and Vector Control Research Lab, Department of Pharmacology, Saveetha Medical College and Hospital, Saveetha Institute of Medical And Technical Sciences (SIMATS), Thandalam, Chennai-602105, Tamil Nadu, India. dass.smc@saveetha.com; kdassrsgc1987@gmail.com; ORCID: https://orcid.org/0000-0002-4564-3275

ABSTRACT

This study presents an eco-friendly synthesis of copper oxide (CuO) nanoparticles using Pocockiella variegata (macroalgae) extracts and their integration into starch/polyvinyl alcohol (PVA) electrospun nanofibrous scaffolds for potential anticancer applications. The synthesized CuO nanoparticles exhibited a characteristic surface plasmon resonance peak at 292 nm, confirming their formation, while Fourier-transform infrared spectroscopy (FTIR) and X-ray diffraction (XRD) analyses validated the presence of Cu–O bonds and a monoclinic crystalline structure. Scanning electron microscopy (SEM) imaging revealed well-dispersed CuO particles within the fibrous scaffold, with sizes ranging from 50–200 nm, and high porosity suitable for biomedical use. Thermal analysis indicated improved thermal stability of the CuO-loaded scaffold compared to native polymers. Dynamic light scattering (DLS) and zeta potential studies confirmed moderate colloidal stability and particle dispersion. In vitro cytotoxicity assays against HT-29 and MCF-7 cancer cell lines showed that the CuO-loaded nanoscaffolds exhibited enhanced anticancer activity with lower IC_{50} values than free nanoparticles or algal extract. These findings suggest the developed nanoscaffold as a promising candidate for cancer therapeutics.

KEYWORDS: *Pocockiella variegata*; Green synthesis; CuO nanoparticles; Starch/PVA/CuO-NPs nanoscaffolds; Anticancer activity

1. INTRODUCTION

Cancer remains a major global health burden, accounting for millions of deaths annually [1]. Among the various types, colorectal cancer (CRC) and breast cancer are among the most prevalent, with high morbidity and mortality rates [2]. Despite advancements in diagnostics and therapeutic strategies, current treatments such as chemotherapy and radiotherapy are often associated with adverse side effects, systemic toxicity, and the emergence of drug resistance [3]. This growing concern has driven researchers to explore alternative and more biocompatible therapeutic platforms, especially those derived from natural sources [4]. Nanotechnology, particularly in the domain of nanomedicine, has shown remarkable promise in the development of novel anticancer agents that offer improved therapeutic indices and reduced side effects [5].

Metal oxide nanoparticles, especially copper oxide nanoparticles (CuO NPs), have emerged as potent therapeutic candidates due to their unique physicochemical properties [6]. CuO NPs possess remarkable biological activity, including antimicrobial, antioxidant, and anticancer effects, attributed to their high surface area-to-volume ratio, redox activity, and ability to generate reactive oxygen species (ROS) [7]. Their therapeutic applications have been further advanced through green synthesis approaches, which offer eco-friendly, sustainable, and less toxic methods of production [8]. The utilization of plant and marine extracts in the biosynthesis of nanoparticles has gained momentum as they provide natural capping, reducing, and stabilizing agents [9]. Among these, marine macroalgae have demonstrated vast potential due to their rich phytochemical composition, including polyphenols, flavonoids, alkaloids, and sulfated polysaccharides [10].

Marine algae, particularly from coastal regions like Rameswaram, India, are a valuable yet underexplored resource for bioactive compounds with pharmacological relevance [11]. *Pocockiella variegata*, a green marine macroalga, has attracted attention owing to its rich content of bioactive constituents [12]. The integration of such algae in the biosynthesis of metal-

based nanoparticles not only enhances the biocompatibility of the final product but also imparts inherent therapeutic properties from the algal metabolites [13]. This synergy of marine biology and nanotechnology offers a novel approach for creating multifunctional nanomaterials with high efficacy in cancer therapeutics [14].

Electrospinning has emerged as a versatile and efficient technique for fabricating nanofibrous scaffolds that closely mimic the extracellular matrix (ECM) of native tissues [15]. These nanofibers provide a conducive microenvironment for cell attachment, proliferation, and differentiation, making them highly suitable for biomedical applications including drug delivery and tissue engineering [16]. Polyvinyl alcohol (PVA) is a commonly used polymer in electrospinning due to its excellent spinnability, biocompatibility, and mechanical strength [17]. When blended with natural polymers like starch, the biocompatibility and biodegradability of the resulting scaffolds are further enhanced [18]. Moreover, incorporating nanoparticles such as CuO NPs into PVA/starch nanofibers provides an additional layer of functionality, enabling the scaffold to serve as a delivery vehicle for anticancer agents while simultaneously contributing to cytotoxicity against cancer cells [19].

Green-synthesized CuO NPs, when embedded into electrospun scaffolds, create a composite material that unites structural support with bioactivity [20]. The porous nature and high surface area of nanofibers facilitate controlled release of embedded nanoparticles, improving the targeted action against cancer cells [21]. Additionally, the inherent therapeutic activity of CuO NPs—amplified by the phytochemicals from *P. variegata*—may enhance the overall cytotoxic potential of the scaffold while minimizing damage to surrounding healthy tissues [22].

The present study focuses on the green synthesis of CuO NPs using *P. variegata* extract and their incorporation into starch/PVA electrospun nanofibrous scaffolds. The synthesized nanocomposite was thoroughly characterized using advanced analytical techniques, including UV–Visible spectroscopy, Fourier-transform infrared spectroscopy (FTIR), X-ray diffraction (XRD), Scanning electron microscopy (SEM), Thermogravimetric analysis (TGA), and Dynamic light scattering (DLS) to elucidate its physicochemical and morphological properties [23]. Furthermore, the in vitro anticancer activity of the algal extract, CuO NPs, and the CuO NP-loaded nanofibers was evaluated using MTT assays against two widely studied cancer cell lines: HT-29 (colorectal adenocarcinoma) and MCF-7 (breast adenocarcinoma) [24]. These cell lines serve as robust models for assessing the cytotoxic efficacy and potential selectivity of novel anticancer formulations [25].

This interdisciplinary research bridges the domains of marine biotechnology, green nanotechnology, and advanced biomaterial engineering to create a promising nanotherapeutic platform [26]. The strategic combination of naturally derived bioactive agents, eco-friendly nanoparticle synthesis, and nanofibrous scaffold fabrication represents a novel and sustainable approach for cancer treatment [27]. By employing a holistic methodology that integrates biosynthetic processes with material science and cell biology, the study aims to develop a biocompatible, efficient, and scalable scaffold system for targeted cancer therapy [28].

Ultimately, the goal of this research is to lay the groundwork for future translational applications of marine-derived nanomaterials in oncology. Given the biocompatibility and bioactivity of the synthesized scaffold, it holds potential not only for in vitro cancer therapy studies but also for future in vivo investigations and clinical translation. Moreover, the use of green synthesis techniques and biodegradable polymers aligns with sustainable development goals, making this approach both scientifically impactful and environmentally responsible.

2. MATERIALS AND METHODS

2.1. Materials

The marine alga *P. variegata* was collected from the coastal waters of Rameswaram, Tamil Nadu, India, for the present study. Copper (II) sulfate pentahydrate (CuSO4·5H2O), procured from Sigma-Aldrich, was utilized as the precursor for synthesizing CuO NPs. PVA (MW 115,000) acted as the polymeric base during electrospinning, while starch sourced locally was incorporated into the nanofiber structure. All analytical-grade reagents and solvents, including Milli-Q water and ethanol, were obtained from Merck and Sigma-Aldrich. Electrospinning was carried out using a HOLMARC HO-NFES-040 high-voltage setup with a syringe pump to generate PVA/CuO NP nanofibers. For material characterization, instruments used included a VIS SPEC V-730 UV-Vis spectrophotometer, Spectrum Two (PerkinElmer) FTIR spectrometer, Bruker D8 Advance X-ray diffractometer, and JSM-IT800 NANO SEM. Additionally, the Malvern Zetasizer Ultra analyzed nanoparticle size and zeta potential, and thermal behavior was assessed via the PerkinElmer TGA 8000 system. Biological evaluations focused on anticancer activity assessments.

2.2. Marine macroalgae collection

P. variegata specimens were gathered from the intertidal zones of Rameswaram, Tamil Nadu. The algal material was first cleaned using tap water to eliminate surface impurities, followed by several washes with distilled water. Approximately 100 grams of clean biomass were cut into small sections and left to air dry under room temperature for 14 days. Once completely desiccated, the dried algal material was finely powdered using a mechanical grinder and stored in a clean, dry container until used in further experiments.

2.3. Ultrasonic-assisted extraction

To extract bioactive constituents, 2 g of powdered *P. variegata* were mixed with 50 mL of Milli-Q water in a sterile 100 mL beaker. The solution underwent ultrasonic treatment using a LABQUEST bath sonicator (Borosil, Serial No. 941032329018) at 60°C for 45 minutes. After sonication, the mixture was filtered using sterile Whatman No. 1 filter paper to remove debris. The filtrate was collected in a sterile container and stored at 10°C. For further experimentation, the aqueous extract was freeze-dried using a lyophilizer, yielding a powdered form for easy incorporation into subsequent procedures [29, 30].

2.4. Green synthesis of CuO NPs

Green synthesis of CuO NPs was achieved by mixing 50 mL of 0.1 M CuSO4·5H2O solution with 10 mL of aqueous algal extract, which was prepared by dissolving 10 mg of freeze-dried extract in 10 mL Milli-Q water, maintaining a 5:1 volumetric ratio. The mixture was magnetically stirred at 650 rpm and heated to 60°C for 2 hours. A visual color change from blue to pale bluish-green confirmed nanoparticle formation. The suspension was then washed thrice with distilled water under identical stirring and thermal conditions to remove residual contaminants. The purified nanoparticle product was subsequently freeze-dried for 48 hours to yield CuO NPs in powder form [31].

2.5. Fabrication of starch/PVA electrospun scaffolds loaded with CuO NPs

To fabricate nanofibers, a 15% (w/w) PVA solution was prepared in distilled water. Into this solution, 100 mg each of starch and biosynthesized CuO NPs were added, followed by thorough stirring at 50°C for 2.5 hours to achieve homogeneity. The polymer blend was subjected to electrospinning using a HOLMARC HO-NFES-040 system fitted with an HMPSKV30 power supply (0–30 kV, 0.5 mA). The prepared solution was loaded into a syringe with a 0.84 mm internal diameter needle. Optimal spinning parameters were established at 11.5 kV applied voltage, 12.3 cm needle-to-collector distance, and 0.4 mL/h flow rate. Nanofibers were continuously collected for 6–8 hours on aluminum foil-covered collectors under ambient conditions [32-34].

2.6. Physicochemical characterization

2.6.1. UV–visible spectroscopy

The optical properties of macroalgal extract, CuO NPs, and CuO NP-infused starch/PVA nanofibers were analyzed using a VIS SPEC V-730 UV-Visible spectrophotometer. Absorbance was measured from 200 nm to 800 nm, with deionized water used as the blank reference [35].

2.6.2. FTIR spectroscopy analysis

FTIR analysis was carried out using the PerkinElmer Spectrum Two spectrometer in ATR mode to examine the chemical bonds present. Samples included the macroalgal extract, biosynthesized CuO NPs, and CuO NP-loaded scaffolds. Each was scanned 64 times over the 4000–400 cm^{-1} range at a 4 cm^{-1} resolution [36].

2.6.3. XRD analysis

XRD was employed to determine the crystalline nature of CuO NPs and nanofiber composites using a Bruker D8 Advance system with CuKα radiation (λ = 1.5406 Å), operated at 40 kV and 40 mA. Data were recorded across 2θ values ranging from 5° to 90° with a step size of 0.029649° [37].

2.6.4. SEM analysis

SEM imaging was performed using a JSM-IT800 NANO SEM (JEOL, Japan) to evaluate morphological features. All samples were sputter-coated with gold to enhance conductivity and image resolution prior to analysis [38].

2.6.5. TGA

Thermal behavior was assessed using a PerkinElmer TGA 8000. Around 5 mg of each sample was heated in aluminum crucibles from ambient temperature to 550°C at a heating rate of 15°C/min under a nitrogen atmosphere. Mass loss was monitored to assess thermal stability [39].

2.6.6. Zeta potential and particle size analysis

The colloidal stability and size of CuO NPs were examined using DLS and electrophoretic mobility with a Malvern Zetasizer Ultra. Data provided information on hydrodynamic diameter and surface charge characteristics of the nanoparticles [40].

All primary data related to the physicochemical analyses can be accessed via Mendeley Data (doi: 10.17632/6tddv74p8k.1).

2.7. In vitro anticancer activity

2.7.1. Cells (HT-29 and MCF-7 cells) procurement and culture

The Human Colon Adenocarcinoma Cell Line (HT-29) and breast cancer cell lines known as Michigan Cancer Foundation-7 (MCF-7) were obtained from the National Center for Cell Science (NCCS) in Pune, India, and grown following the provided cell culture guidelines. These cells were nurtured in Minimum Essential Medium (MEM) supplemented with 10% FBS at 37˚C in a 5% CO2 atmosphere [41].

2.7.2. Cell viability assessment by MTT

HT-29 and MCF-7 cells were seeded in 96-well plates at a concentration of 5 x 105 cells per well and allowed to attach overnight. Subsequently, the cells were treated with different concentrations of algal extract, CuO NPs and starch/PVA/CuO-NPs nanoscaffolds with varying concentrations (6.25, 12.5, 25, 50, and 100 µg/mL) in triplicates and placed in a 37˚C incubator with 5% CO2 for 24 hours. After the incubation period, each well was supplemented with MTT solution and further incubated at 37°C for 4 hours. The formazan crystals formed were dissolved in 200 µl of dimethyl sulfoxide (DMSO). The optical density (OD) of the resulting solution was measured at 570 nm using a spectrophotometer. This experiment was repeated three times independently to ensure reliability. The mean OD and standard deviation were calculated for each set of replicates, providing a comprehensive analysis of the results obtained [42].

2.8. Statistical analysis

All experimental data were statistically analyzed using SPSS version 25.0 and GraphPad Prism version 9.0 software. Results from triplicate experiments were presented as mean ± standard deviation. Differences between groups were evaluated using one-way analysis of variance (ANOVA), followed by suitable post-hoc comparisons, such as Tukey's or

Dunnett's test, where applicable. A significance level of $p < 0.05$ was considered statistically meaningful. Pearson's correlation coefficient was used to examine relationships between variables. The Shapiro–Wilk test was performed to assess data normality, and datasets failing normality assumptions were subjected to logarithmic transformation. All interpretations were made within a 95% confidence interval to maintain the integrity of statistical outcomes[43].

3. RESULTS

3.1. UV–visible spectroscopy

The UV–Vis absorption profile of the macroalgae-derived extract (Figure 1) displayed a significant peak at 267 nm with a maximum absorbance of 0.4035, indicating the presence of UV-active secondary metabolites, including aromatic or phenolic compounds with extended conjugation. The overall absorbance spanned between 0.3285 and 0.4035 across the 200–800 nm spectrum. Minimal activity in the visible range (400–700 nm) suggested low chlorophyll content, possibly due to degradation or extract purification. In comparison, the biosynthesized CuO NPs showed a distinctive surface plasmon resonance (SPR) peak at 292 nm and a higher absorbance of 0.70716. This blue shift from the conventional CuO SPR range (570–600 nm) likely resulted from nanoparticle downsizing, surface oxidation, or phytochemical-assisted stabilization during synthesis. The CuO NPs demonstrated absorbance between 0.31409 and 0.70716, and the steep decline after the peak implied the formation of uniformly distributed particles with limited aggregation.

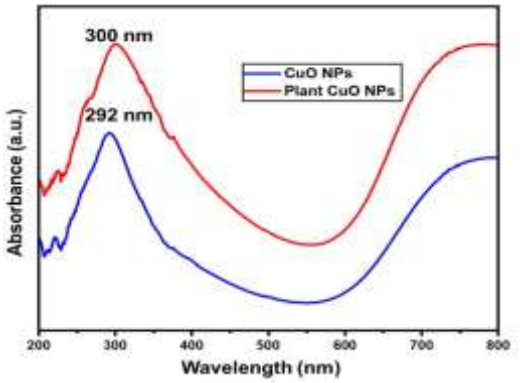

Figure 1: UV–Visible Spectroscopy analysis of algae extract and CuO NPs

3.2. FTIR spectroscopy analysis

FTIR spectral analysis (Figure 2) of the green-synthesized CuO NPs revealed the functional moieties involved in both synthesis and surface capping. A broad signal at 3219.71 cm^{-1} indicated –OH and N–H stretches, attributable to phytochemical agents functioning as stabilizers. Peaks observed near 1509.94 cm^{-1} and in the 672–463 cm^{-1} region corresponded to aromatic ring structures and Cu–O bond vibrations, respectively, validating CuO NP generation. Spectra of the starch/PVA scaffold showed typical polymer signatures, including an –OH stretch at 3295.71 cm^{-1}, C–H stretches at 2923.65 cm^{-1}, and ether (C–O–C) bonds between 1141–1088 cm^{-1}. Overlapping signals in the 605–478 cm^{-1} range denoted embedded CuO particles within the matrix. A shift in the hydroxyl peak implied hydrogen bonding interactions between the CuO NPs and the polymer matrix, enhancing structural integrity. Additionally, a carbonyl peak at 1711.09 cm^{-1} likely indicated either oxidation of PVA or bonding between CuO and the C=O group of PVA.

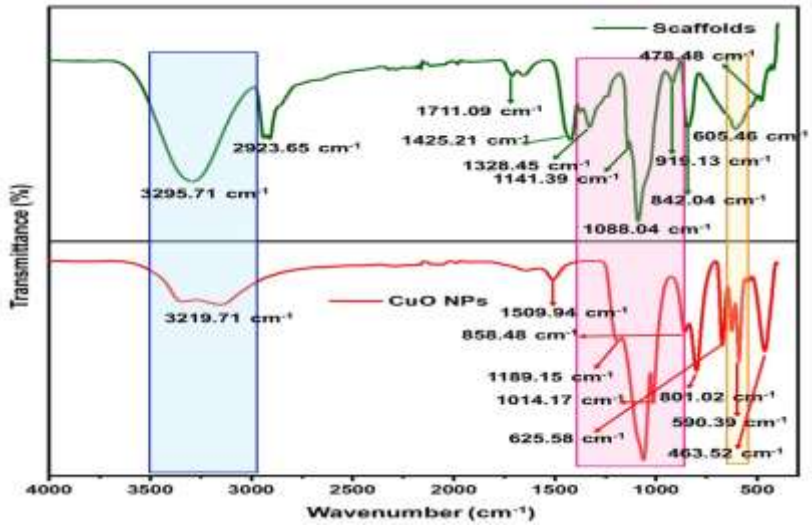

Figure 2: FTIR analysis of CuO NPs and nanoscaffolds

3.3. XRD analysis

XRD analysis (Figure 3) of the biosynthesized CuO NPs and CuO-loaded starch/PVA scaffolds revealed definitive crystalline patterns. CuO NPs displayed intense reflections at 2θ values of 32.75°, 35.70°, 38.05°, 48.66°, 57.94°, 61.33°, and 75.48°, with corresponding d-spacings from 1.59 to 3.67 Å, matching monoclinic CuO per JCPDS 48-1548, with no

evidence of Cu_2O impurities. The prominent peak at 35.70° (002)/(111) recorded a net area of 141.86 Cps × °. Crystal sizes ranged from 20–50 nm as estimated using Scherrer's formula with FWHM between 0.1°–0.9°. The polymer scaffold exhibited broader reflections at 21.35°, 22.97°, and 43.14° 2θ, confirming its semi-crystalline nature. CuO peaks at 35.70°, 57.28°, and 61.33° were diminished, suggesting nanoparticle encapsulation. A wide amorphous band between 10°–30° and lower FWHM values (0.16°–1.06°) pointed to enhanced nanoparticle dispersion due to the polymer matrix. A negative net intensity observed at 39.46° may stem from instrumental errors. Collectively, the findings confirmed effective nanoparticle formation and uniform integration within the scaffold, suitable for biomedical application.

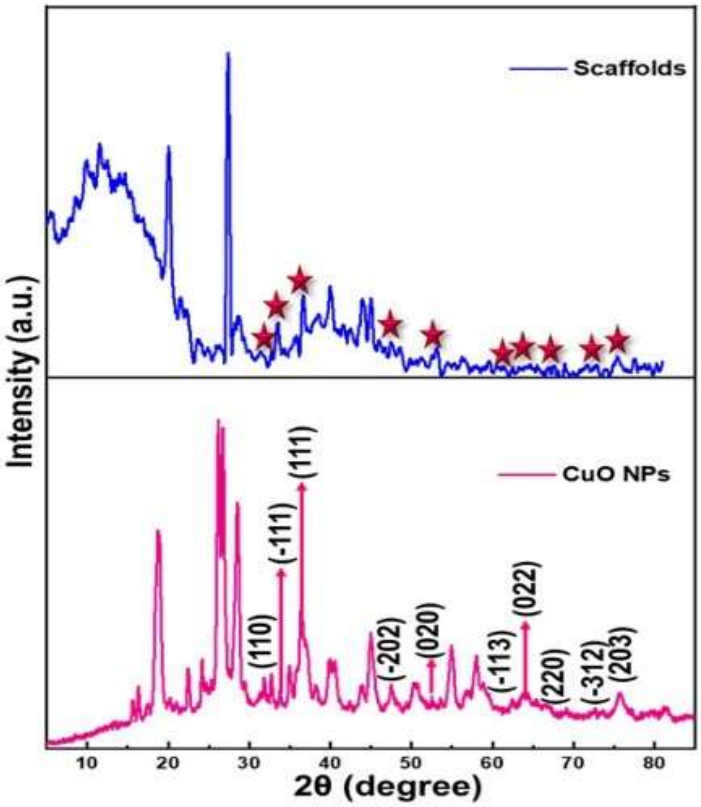

Figure 3: XRD analysis of CuO NPs and nanoscaffolds

3.4. SEM analysis

SEM imaging (Figure 4), performed using gold-coated JSM-IT800 NANO SEM, displayed biosynthesized CuO NPs with morphologies varying from round to irregular shapes, ranging in size from 50–200 nm. Some clusters, measuring between 500–1000 nm, were noted and could be attributed to electrostatic interactions and partial agglomeration. The particles appeared rough-surfaced, likely due to phytochemical coatings from the macroalgal extract. Electrospun starch/PVA nanoscaffolds embedded with CuO revealed a consistent fibrous network devoid of bead formation, with fiber diameters ranging from 150–300 nm. The structure showed high porosity, ideal for biomedical roles such as tissue engineering or wound healing. Fine bright particles (<200 nm) distributed along the fibers suggested that CuO NPs were well-dispersed and securely integrated, retaining scaffold uniformity and mechanical integrity.

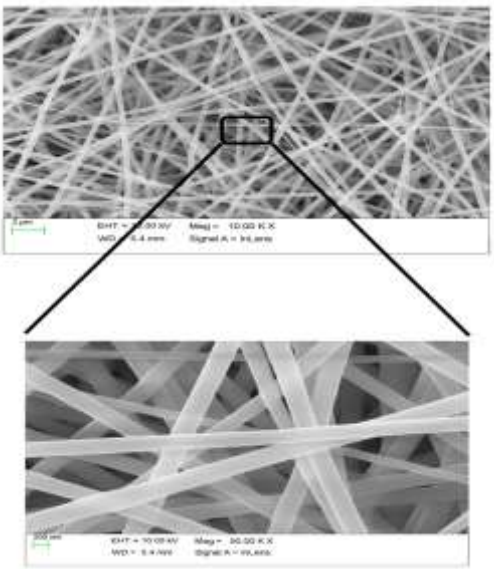

Figure 4: SEM analysis of starch/PVA/CuO-NPs nanoscaffolds

3.5. TGA

Thermal stability of the CuO-incorporated starch/PVA scaffolds was evaluated through TGA in a nitrogen atmosphere (Figure 5), revealing a total weight loss of 35.87% and a retained mass of 64.13%, primarily due to CuO and other thermally stable elements. Degradation proceeded in three phases: the first phase (50–90°C) corresponded to water loss, showing a maximum degradation rate of -2.54%/min at 53.71°C. The main degradation stage initiated at 262.78°C and peaked at 326.36°C, marked by breakdown of the polymer's backbone (C–C and C–O bond cleavage), reaching a peak rate of -2.93%/min. The last phase ended at 363.12°C, involving residual carbon decomposition. In comparison, native starch/PVA scaffolds degraded below 250°C. The inclusion of CuO delayed thermal breakdown and reduced overall mass loss, confirming that nanoparticles enhanced thermal resilience an essential property for biomedical systems requiring sterilization or heat exposure

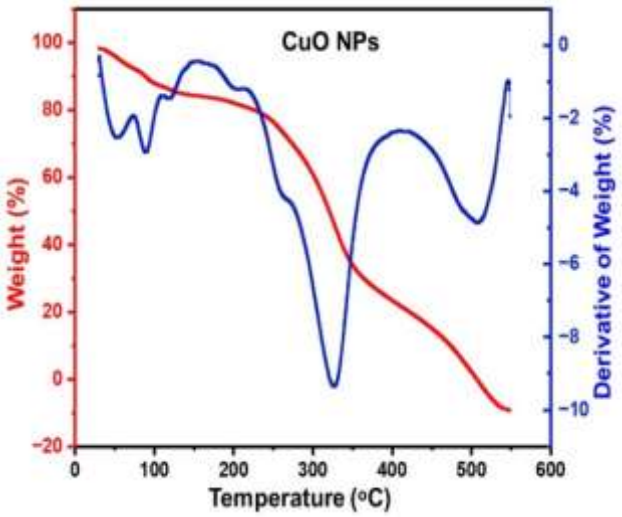

Figure 5: TGA analysis of starch/PVA electrospun nanoscaffolds

3.6. Zeta potential and particle size analysis

DLS measurements of the aqueous CuO NP suspension at 25°C recorded a Z-average hydrodynamic size of 125.6 nm (Figure 6) with a polydispersity index (PI) of 0.475, indicating moderate heterogeneity. Size distribution revealed three peaks: the main peak at 881.5 nm (84.89% intensity), a secondary one at 128.3 nm (12.06%), and a minor peak at 5350 nm (3.06%), reflecting partial agglomeration (Figure 7). Zeta potential, measured via electrophoretic light scattering, was -10.03 mV, which falls below ±30 mV, suggesting only moderate colloidal stability due to limited repulsive forces. However, steric stabilization from surface-bound phytochemicals likely contributed to maintaining dispersion. Other parameters included conductivity of 0.1813 mS/cm, dispersant viscosity of 0.887 cP, and a dielectric constant of 78.5. The quality factor of 1.754 and stable phase behavior confirmed data accuracy. Nonetheless, surface functionalization or the use of stabilizing additives may be required to improve long-term dispersion for biomedical applications.

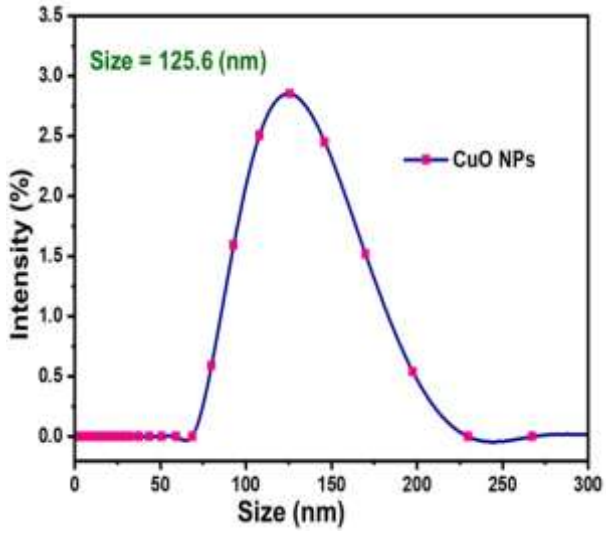

Figure 6: DLS particle size analysis of CuO NPs

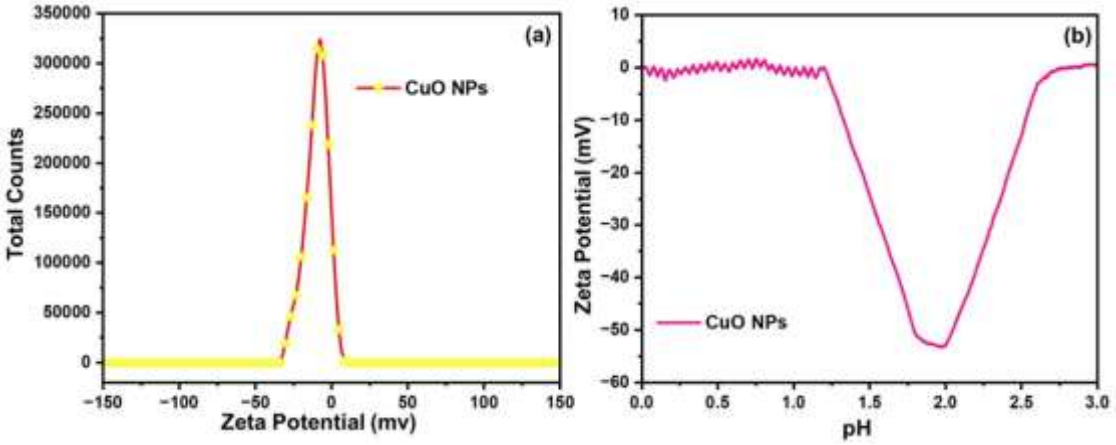

Figure 7: Zeta potential analysis of CuO NPs

2.7. In Vitro anticancer activity analysis

The MTT assay (Figure 8) on HT-29 cells revealed dose-dependent cytotoxicity for algal extract, CuO NPs, and starch/PVA/CuO-NPs nanoscaffolds. The algal extract reduced viability from 94.7% (6.25 µg/mL) to 33.45% (100 µg/mL), CuO NPs from 79.7% to 23.03%, and nanoscaffolds from 76.1% to 16.08%, with IC50 values of ~35 µg/mL, ~20 µg/mL, and ~15 µg/mL, respectively, indicating the nanoscaffolds as the most potent.

Similar trends were observed in MCF-7 cells, where the algal extract decreased viability from 95.3% to 46.05%, CuO NPs from 84.8% to 37.47%, and nanoscaffolds from 78.4% to 24.42%, with IC50 values of ~45 µg/mL, ~30 µg/mL, and ~22 µg/mL, respectively, further confirming the superior efficacy of the nanoscaffolds. The nanoscaffolds consistently exhibited the highest cytotoxicity in both cell lines, followed by CuO NPs and the algal extract, suggesting enhanced therapeutic potential due to synergistic effects, warranting further investigation for cancer treatment applications.

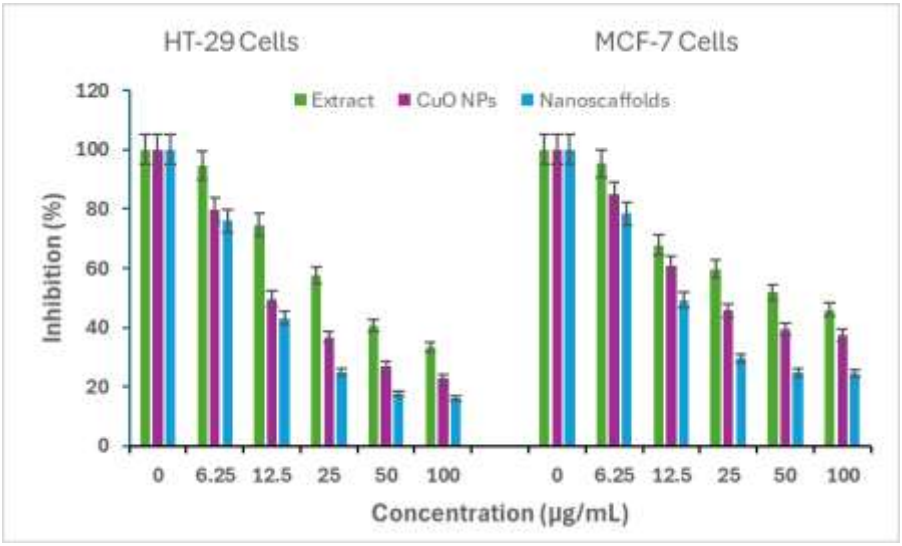

Figure 8: Anticancer potential of algal extract, CuO NPs and starch/PVA/CuO-NPs nanoscaffolds

4. DISCUSSION

The current study presents a comprehensive characterization of CuO NPs synthesized using macroalgal extract, their integration into starch/PVA scaffolds, and the evaluation of their physicochemical and biological properties. The successful fabrication and functionalization of these nanocomposite scaffolds are validated through multiple analytical techniques, each of which provides critical insights into the scaffold's composition, stability, morphology, and therapeutic potential.

The UV–Visible spectroscopy results provide initial confirmation of both the presence of bioactive compounds in the macroalgal extract and the successful synthesis of CuO NPs. The algal extract exhibited a peak at 267 nm, which is characteristic of phenolic or aromatic compounds possessing extended conjugated systems. This implies that these phytochemicals may play a dual role—as reducing and capping agents during nanoparticle formation. Notably, the CuO NPs exhibited a strong absorption peak at 292 nm, which indicates a blue shift from the typical range of CuO surface plasmon resonance (SPR) peaks. This shift may be attributed to the reduction in particle size and the influence of bioorganic molecules from the extract that could alter the electronic environment of the nanoparticles. The sharp decline in absorbance post-peak also suggests uniform particle size distribution and minimal aggregation, crucial attributes for biomedical nanomaterials [44].

Further molecular-level validation was provided by FTIR spectroscopy, which confirmed the involvement of various functional groups in nanoparticle synthesis and scaffold formation. In CuO NPs, broad absorption bands associated with –OH and N–H stretching vibrations highlight the presence of bio-organic molecules on the nanoparticle surface, reinforcing the phytochemical-assisted synthesis mechanism. The appearance of Cu–O stretching bands and aromatic ring vibrations further substantiated the formation of CuO. The FTIR spectra of the starch/PVA/CuO scaffold displayed characteristic polymer peaks, such as –OH stretching, C–H bending, and C–O–C ether linkages. Importantly, shifts and overlaps in these bands upon nanoparticle incorporation suggest interactions like hydrogen bonding between the polymer matrix and nanoparticles, potentially improving mechanical stability and functional performance [45].

XRD analysis provided structural confirmation of nanoparticle crystallinity and polymer-nanoparticle interaction. The CuO NPs displayed distinct peaks aligned with monoclinic CuO crystal structures, with no sign of Cu_2O or other metallic impurities, ensuring phase purity. The sharp peak at 35.70° and its corresponding d-spacing reaffirm the crystalline nature and small grain size of the nanoparticles (20–50 nm), as calculated via the Scherrer equation. Conversely, the polymeric scaffold exhibited broader peaks, indicative of its semi-crystalline nature. The reduction in intensity of the CuO-related peaks in the composite scaffolds further confirmed the successful encapsulation and homogeneous dispersion of nanoparticles within the polymeric matrix [46].

SEM analysis elucidated the morphology and surface characteristics of the synthesized materials. CuO NPs were predominantly spherical to irregular in shape and measured between 50–200 nm, though some agglomerates up to 1000 nm were observed, likely due to van der Waals forces or electrostatic interactions. The starch/PVA/CuO nanofibrous scaffolds demonstrated a uniform fibrous network with no bead formation, and fiber diameters ranged from 150–300 nm. The presence of bright dots on the fiber surfaces suggested that the CuO NPs were successfully embedded within the scaffold structure without disrupting the overall fiber morphology. The high porosity of the scaffold also makes it a strong candidate for applications such as tissue engineering or drug delivery [47].

Thermal stability, an essential parameter for biomedical applications, especially under sterilization conditions, was assessed via TGA. The starch/PVA/CuO nanoscaffold exhibited a three-phase degradation profile with an overall weight loss of 35.87%, indicating significant thermal stability. The onset of major degradation was observed above 260°C, with maximum degradation rates around 326°C, far higher than the native starch/PVA scaffold. The enhanced thermal stability can be attributed to the incorporation of thermally stable CuO NPs, which likely act as heat dissipation centers, delaying polymer breakdown and supporting their application in temperature-sensitive environments[48].

Zeta potential and DLS measurements offered insights into nanoparticle dispersion and colloidal stability. The CuO NPs had a hydrodynamic diameter of 125.6 nm and a polydispersity index of 0.475, indicating moderate size variation. The zeta potential of -10.03 mV suggests modest colloidal stability, which may be sufficient for short-term applications but could benefit from additional surface modification to enhance long-term dispersion. The presence of multiple peaks in the DLS analysis further hinted at some degree of nanoparticle aggregation, a common issue in green-synthesized nanoparticles [49].

Biological evaluation using MTT assays revealed compelling anticancer activity. The algal extract, CuO NPs, and the composite scaffold all demonstrated dose-dependent cytotoxicity against HT-29 and MCF-7 cancer cell lines. Among them, the nanoscaffolds exhibited the highest cytotoxic effect, with IC50 values of approximately 15 µg/mL (HT-29) and 22 µg/mL (MCF-7), outperforming both the nanoparticles and extract alone. This enhanced activity may stem from a synergistic interaction between the CuO NPs and the bioactive phytochemicals retained in the scaffold. The fibrous structure might also contribute to sustained release and improved cellular interaction, intensifying cytotoxic effects [50].

The integration of biosynthesized CuO NPs into a starch/PVA scaffold has resulted in a multifunctional nanocomposite with promising structural, thermal, and biological properties. The scaffold's excellent thermal stability, high porosity, and potent anticancer activity position it as a viable candidate for advanced biomedical applications, particularly in cancer therapy and tissue engineering. Further studies, including in vivo evaluations and long-term biocompatibility assessments, are essential to translate these findings into clinical potential.

5. CONCLUSION

This study successfully demonstrated the green synthesis of CuO NPs using macroalgae-derived extracts and their effective incorporation into starch/PVA electrospun nanofibrous scaffolds. Characterization through UV–Vis, FTIR, XRD, SEM, TGA, and zeta potential analysis confirmed the formation of stable, well-dispersed nanoparticles with promising physicochemical properties. The CuO NPs exhibited significant crystallinity, thermal stability, and moderate colloidal behavior, while integration into the starch/PVA matrix resulted in a porous, fibrous scaffold with enhanced structural integrity. Most notably, the in vitro cytotoxicity studies against HT-29 and MCF-7 cancer cell lines revealed potent, dose-dependent anticancer activity, with the nanoscaffolds outperforming both free CuO NPs and algal extracts. These findings highlight the synergistic therapeutic potential of the developed nanoscaffold system, positioning it as a promising candidate for further exploration in targeted cancer therapy. Future research may focus on in vivo validation, controlled drug release behavior, and biosafety profiling to advance clinical applicability.

Ethical Declaration: Not applicable for this study.

Funding: Not available for this study.

Conflicts of Interest: The authors declare no conflicts of interest.

Data Availability Statement: The full dataset of physiochemical characterization associated with this work is published in Mendeley Data [Dataset] Physiochemical characterization of fabricated starch-based nanoscaffolds incorporated with *Pocockiella variegata* extract-mediated green synthesised copper oxide nanoparticles (DOI: 10.17632/6tddv74p8k.1).

Disclosure: The material characterization data and figures (e.g., UV, SEM, FTIR, XRD, TGA, Zeta Potential and particle sizer) presented here were generated from a common dataset and are being reused across multiple related studies on nanomaterials. All biological analyses and conclusions are original to each manuscript.

REFERENCES

1. Surendran N, Chandrasekaran G, Raju MV, Chandrasekaran MK, Ahalliya RM, Palanisamy CP, Kanniappan GV, Arcot R, Alharbi NS, Thiruvengadam M. Anti-inflammatory potential of ethanolic extract of Maranta arundinacea L.: Insights from COX-2 modulation and oxidative stress analysis. South African Journal of Botany. 2026; 195: 142-151.
2. Pei J, Senthilkumar MV, Hessini K, Subramaniyam S, Sivaramakrishnan R, Kanniappan GV, Jayaraman S, Palanisamy CP. Green fabrication of starch/PVA/CuO nanoscaffolds using marine macroalgae extract for enhanced anti-inflammatory activity. Sustainable Chemistry and Pharmacy. 2026; 51: 102397.
3. Balasubramanian V, Loganathan L, Muthuswamy K, Viswanathan TM, Raju MV, Chandrasekaran MK, Ahalliya RM, Poorasamy J, Palanisamy CP, Dominic S, Kanniappan GV. Anticancer therapeutic efficacy of PEGylated β-galactosidase from Aspergillus terreus in DMBA-induced breast cancer: Toxicological, molecular and histopathological evaluation in Wistar rats. International Journal of Biological Macromolecules. 2026; 360: 151856.
4. Jayaraman S, Eswaran A, Rajagopal P, Palanisamy CP, Veerakumar P, Veeraraghavan VP, Sirasanagandla SR. Neuroendocrine-associated epigenetic factors in cellular senescence: mechanisms and therapeutic implications. Biogerontology. 2026; 27(2): 64.
5. Ponnusamy B, Rajagopal P, Palanisamy CP, Veeraraghavan VP, Jayaraman S. Mechanistic Exploration of the anticancer activity of Justicia adhatoda Plant Leaf Ethanolic Extract against Colon Cancer Cells: An in silico and in vitro Approach. Asian Pacific Journal of Cancer Prevention. 2026; 27(3): 1069-1080.
6. Pei J, Saran VS, Sivaramakrishnan R, Kanniappan GV, Pandurangan V, Jayaraman S, Dhayalan VK, Mironescu M, Mironescu ID, Palanisamy CP. Ultrasonic-assisted, Sargassum ilicifolium (brown marine macroalgae)-mediated biogenic synthesis of CuO nanoparticles incorporated in starch/PVA electrospun nanoscaffolds: In vitro safety and antioxidant efficacy assessment. Bioorganic Chemistry. 2026; 173: 109679.
7. Raj MAPA, Subramaniyam S, Kanniappan GV, Jayaraman S, Palanisamy CP. Sustainable fabrication of starch/PVA/CuO electrospun nanoscaffolds from Turbinaria ornata (marine macroalgae) extract: Physicochemical characterization and antidiabetic evaluation. Kuwait Journal of Science. 2026; 53(2): 100545.
8. Pei J, Ganesh NS, Subramaniyam S, Sivaramakrishnan R, Kanniappan GV, Jayaraman S, Palanisamy CP. Sustainable fabrication of starch/PVA/CuO electrospun nanoscaffolds from Padina tetrastromatica (Brown macroalgae) extract: Physicochemical characterization and antidiabetic assessment. Sustainable Chemistry One World. 2026; 9: 100195.
9. Sakthiraj A, Sivaramakrishnan R, Subramaniyam S, Kanniappan GV, Pandurangan V, Jayaraman S, Dhayalan VK, Mironescu M, Mironescu ID, Palanisamy CP. Chemical Physics Impact. Starch/PVA electrospun nanoscaffolds loaded with ultrasonic-assisted green-synthesis of CuO nanoparticles from marine macroalgae (Gracilaria corticata) extract: Cytotoxicity and antioxidant analysis. 2026; 12: 101018.
10. Raju M, Chandrasekaran MK, Loganathan L, Ahalliya RM, Mironescu M, Mironescu ID, Palanisamy CP, Kanniappan GV. Lipid remodeling and ferroptosis in phosphatidylcholine-mediated tumor–stroma crosstalk. Frontiers in Molecular Biosciences. 2026; 13: 1742305.
11. Kunamalla R, Panagal M, Palanisamy CP. Biogenic synthesis and fabrication of starch/PVA/CuO electrospun nanoscaffolds from Sargassum ilicifolium (brown marine macroalgae) extract for anticancer activity on HT-29 and MCF-7 cancer cells. Biocatalysis and Agricultural Biotechnology. 2026; 72: 103923.
12. Pei J, Govindaraj H, Sivaramakrishnan R, Kanniappan GV, Pandurangan V, Dhayalan VK, Mironescu M, Mironescu ID, Jayaraman S, Palanisamy PC. Sustainable fabrication of biopolymer-based (starch/PVA) nanoscaffolds loaded with green-synthesized CuO nanoparticles from Sargassum wightii (marine macroalgae): Cytocompatibility and antioxidant activity. Biomaterials Advances. 2026; 182: 214660.
13. Pei J, Perumal NC, Meng P, Long Q, Palanisamy CP. Extracellular vesicle-based biosensors for Alzheimer's disease: A new frontier in precision diagnostics. Ageing Research Reviews. 2026; 113: 102904.
14. Shree P, Sivaramakrishnan R, Kanniappan GV, Pandurangan V, Jayaraman S, Dhayalan VK, Mironescu M, Mironescu ID, Palanisamy CP. Antioxidant and biocompatible CuO-starch/PVA nanoscaffolds via ultrasonic green synthesis using Turbinaria conoides (brown marine macroalgae). Medicine in Drug Discovery. 2025; 28: 100238.
15. Gong J, Lin J, Guan T, Pei J, Palanisamy CP, El-AtyFrom AMA. selenium tolerance to nanoplastic antagonism: Comprehensive characterization of L. casei SNUT1 and its extracellular vesicle–nanoselenium complex. Food Bioscience. 2025; 74: 107749.
16. Poochi SP, Sundarraj R, Raju MV, Chandrasekaran MK, Ahalliya RM, Palanisamy CP, Kanniappan GV, Kondapavuluri BK, Thiruvengadam M. Harnessing Nature: Computational and Experimental Insights Into Ipomoea obscura Metabolites for Bladder Cancer Therapy. Chemistry and Biodiversity. 2025; 0: e00909.
17. Dugganaboyana GK, Kannankumar MKG, Shivaramakrishna S, Raju MV, Chandrasekaran MK, Ahalliya RM, Panneerselvam N, Palanisamy CP, Kanniappan GV. Phytochemical insights, antioxidant activity and therapeutic potential of Cassia senna against prostate cancer in Wistar albino rats. Discover Applied Sciences. 2025; 7:1206.
18. Natarajan SR, Krishnamoorthy R, Alshuniaber MA, Gatasheh MK, Rajagopal P, Veeraraghavan VP, Palanisamy CP, Jayaraman S. KDM1A Facilitates Oncogenic Potential in Colorectal Cancer Progression Through the Activation of

AXIN/GSK3β/β-Catenin Signaling Pathways: Evidence From Integrated Transcriptomics and In Vitro Studies. The Journal of Gene Medicine. 2025; 27(11): e70053.
19. Guan T, Gong J, Lin J, Palanisamy CP, Jinjin Pei J, El-Aty AMA. Machine learning-driven multimodal optimization of selenium biotransformation and flavor profiling in fermented apple–Yacon functional beverages. Innovative Food Science & Emerging Technologies. 2025; 105: 104198.
20. Natarajan SR, Krishnamoorthy R, Alshuniaber MA, Alsulami TS, Gatasheh MK, Rajagopal P, Palanisamy CP, Govindan R, Veeraraghavan VP, Jayaraman S. ABCE1 facilitates tumour progression via aerobic glycolysis and inhibits cell death in human colorectal cancer cells through the p53 signalling pathway. Scientific Reports. 2025; 15: 24674.
21. Huang Y, Guo H, Liu Y, Jin W, Palanisamy CP, Pei J, Oz F, El-Aty AMA. Effects of Natural Polysaccharides on the Gut Microbiota Related to Human Metabolic Health. Molecular Nutrition & Food Research. 2025; 69:e202400792.
22. Poornima K, Meenakshi K.C, Manikandan V.R, Shankari G, Prabhu D, Rathi M.A, Palanisamy CP, Balaji R, Gopalakrishnan V.K. Exploring the anticancer potential of Jerantinine A from Tabernaemontana coronaria against prostate, breast, and ovarian cancers: A computational approach. Journal of Complementary and Integrative Medicine, 2025 22(2): 363–372.
23. Palanisamy CP, Poompradub S, Sansanaphongpricha K, Jayaraman S, Subramani K. Faridah Sonsudin gGreen synthesis of Nigella sativa-mediated silver nanoparticles for enhanced antibacterial activity and wound healing: Mechanistic insights and biomedical applications. Environmental Nanotechnology, Monitoring & Management. 2025; 24: 101085.
24. Surendran N, Raju MV, Chandrasekaran MK, Ahalliya RM, Palanisamy CP, Chandrasekaran G, Kanniappan GV. Physicochemical characterization of starch from Maranta arundinacea L.(arrowroot) rhizomes and its inhibition of COX-2: In vivo validation. Bioactive Carbohydrates and Dietary Fibre. 2025; 33: 100465.
25. Kannappan P, Chandrasekaran MK, Raju MV, Gopalakrishnan S, Dhamodharan P, Ahalliya RM, Palanisamy CP, Raju B, Kanniappan GV. Exploring the anticancer potential of Jerantinine A from Tabernaemontana coronaria against prostate, breast, and ovarian cancers: a computational approach. Journal of Complementary and Integrative Medicine. 2025; 22(02): 363-372.
26. Pei J, Kumarasamy RV, Jayaraman S, Kanniappan GV, Long Q, Palanisamy CP. Quercetin-functionalized nanomaterials: Innovative therapeutic avenues for Alzheimer's disease management. Ageing Research Reviews. 2025; 104: 102665.
27. Jayaraman S, Prasad M, Natarajan SR, Krishnamoorthy R, Alshuniaber MA, Gatasheh MK, Veeraraghavan VP, Rajagopal P, Palanisamy CP. Molecular mechanisms underlying the effects of beta-sitosterol on TGF-β1/Nrf2/SIRT1/p53-mediated signaling in the kidney of a high-fat diet and sucrose-induced type-2 diabetic rat. Chemico-Biological Interactions. 2025; 411: 111443.
28. Huang Y, Guo H, Liu Y, Jin W, Palanisamy CP, Pei J, Oz F, El-Aty AMA. Effects of Natural Polysaccharides on the Gut Microbiota Related to Human Metabolic Health. Molecular Nutrition & Food Research. 2025; e202400792.
29. Prabhakaran P, Palanisamy CP, Shanmugam A, Damodharan P, Swaminathan H, Devaraj D, Ahalliya RM, Kanniappan GV. Isolation, structural characterization, and molecular docking studies on the bioactive compound from n-Hexane extract of Emilia sonchifolia (L.) DC against the pancreatic cancer target Aurora 2 Kinase. Journal of Complementary and Integrative Medicine. 2024; 22(1): 0290.
30. Jiang H, Kumarasamy RV, Pei J, Raju K, Kanniappan GV, Palanisamy CP. Integrating engineered nanomaterials with extracellular vesicles: Advancing targeted drug delivery and biomedical applications. Frontiers in Nanotechnology. 2024; 6: 1513683.
31. Guo H, Liu Y, Wan T, Song D, Palanisamy CP, Geng J, Pei J, Özmen S, El-Aty AMA. Toward personalized cancer management: Role of precision nutrition–diet interventions. Journal of Functional Foods. 2024; 123: 106584.
32. Natarajan SR, Krishnamoorthy R, Alshuniaber MA, Al-Anazi KM, Farah MA, Rajagopal P, Palanisamy CP, Veeraraghavan VP, Jayaraman S. Identification of FOXM1 as a novel protein biomarker and therapeutic target for colorectal cancer progression: Evidence from immune infiltration and bioinformatic analyses. International Journal of Biological Macromolecules. 282 (Part 4): 137201.
33. Rajendran MS, Jayaraman S, Khan JM, Jasmine S, Prabhakaran RK, Raju MV, Chandrasekaran MK, Ahalliya RM, Kannappan P, Palanisamy CP, Kanniappan GV. Investigating the colon toxicity and carcinogenic role of monosodium glutamate compared with Dimethylhydrazine in male Wistar rats: Exploring the link to childhood colon cancer risk. Journal of King Saud University - Science. 2024; 36(11): 103507.
34. Kumarasamy RV, Natarajan PM, Umapathy VR, Roy JR, Rab SO, Saeed M, Panagal M, Mironescu M, Srinivasan GP, Palanisamy CP. Clinical Applications and Therapeutic Potentials of Advanced Nanoparticles: A Comprehensive Review on Completed Human Clinical Trials. Frontiers in Nanotechnology. 2024; 6:1479993.
35. Jin W, Pei JJ, Roy JR, Jayaraman S, Ahalliya RM, Kanniappan GV, Mironescu M, Palanisamy CP. Comprehensive review on single-cell RNA sequencing: A new frontier in Alzheimer's disease research. Ageing Research Reviews. 2024; 274: 102454.
36. Pei J, Palanisamy CP, Jayaraman S, Natarajan PM, Umapathy VR, Roy JR, Panagal M, Jayaraman S. Curcumin-loaded polymeric nanomaterials as a novel therapeutic strategy for Alzheimer's disease: A comprehensive review. Ageing Research Reviews. 2024; 99: 102393.
37. Pei J, Palanisamy CP, Jayaraman S, Natarajan PM, Umapathy VR, Roy JR, Thalamati D, Ahalliya RM, Kanniappan GV*, Mironescu M. A comprehensive review on starch-based Sustainable Edible Films Loaded with Bioactive Components for Food Packaging. International Journal of Biological macromolecules. 2024; 274 (Part-1): 133332.

38. Palanisamy CP, poompradub S, Sansanaphongpricha K, Subramani K, Sonsudin F. Increased expression levels of PDGF and VEGF magnify the wound healing potential facilitated by biogenic synthesis of silver nanoparticles. Nano-Structures & Nano-Objects. 2024; 39: 101236.
39. Pei J, Palanisamy CP, Jayaraman S, Natarajan PM, Umapathy VR, Roy JR, Thalamati D, Ahalliya RM, Kanniappan GV, Mironescu M. Proteomics Profiling of Extracellular Vesicle for Identification of Potential Biomarkers in Alzheimer's Disease: A Comprehensive Review. Ageing Research Reviews. 2024; 99: 102359.
40. Xi J, Wang T, Xian P, Liu X, Du M, Yang H, Palanisamy CP, Lin W, Long Q. Proteomic insights uncover enhanced neurotherapeutic potential in conditioned mesenchymal stem cell-derived extracellular vesicles. Extracellular Vesicle. 2024; 3: 100037.
41. Pei J, Natarajan PM, Umapathy VR, Swamikannu B, Sivaraman NM, Krishnasamy L, Palanisamy CP. Advancements in the synthesis and functionalization of zinc oxide-based nanomaterials for enhanced oral cancer therapy. Molecules. 2024; 29(11): 2706.
42. Gatasheh MK, Natarajan SR, Krishnamoorthy R, Alsulami TS, Rajagopal P, Palanisamy CP, Veeraraghavan VP, Jayaraman S. Molecular analysis to identify novel potential biomarkers as drug targets in colorectal cancer therapy: an integrated bioinformatics analysis. Molecular and Cellular Oncology. 2024; 11(1): 2326699.
43. Pei J, Yan Y, Jayaraman S, Rajagopal P, Natarajan PM, Umapathy VR, Gopathy S, Roy JR, Sadagopan CS, Thalamati D, Palanisamy CP, Mironescu M. A review on advancements in the application of starch-based nanomaterials in biomedicine: Precision drug delivery and cancer therapy. International Journal of Biological Macromolecules. 2024; 130746.
44. Pei JJ, Yan Y, Palanisamy CP, Jayaraman S, Natarajan PM, Umapathy VR, Gopathy S, Roy JR, Sadagopan JC, Thalamati D, Mironescu M. Materials-based drug delivery approaches: Recent advances and future perspectives. Green Processing and Synthesis. 2024; 13: 20230094.
45. Panneerselvam S, Viswaja K, Deepa E, Prathiba S, Rebecca FS, Nivedha RP, Rajagopal P, Veeraraghavan VP, Sridevi G, Palanisamy CP, Jayaraman S. Hypoglycemic Potential of Acalypha indica in Streptozotocin-Induced Type 2 Diabetic Rats. International Journal of Drug Delivery Technology. 2026; 16(26s):1038-1047.
46. Panneerselvam S, Viswaja K, Prathiba S, Rebecca FS, Nivedha RP, Rajagopal P, Fathima SJH, Veeraraghavan VP, Sridevi G, Palanisamy CP, Jayaraman S. Acalypha Indica Attenuates Insulin Resistance in STZ-Induced Type 2 Diabetic Male Rats: Mechanistic Study. International Journal of Drug Delivery Technology. 2026; 16(26s):1027-1037.
47. Manju NE, Natarajan A, Rebecca FS, Nivedha RP, Hemalatha R, Rajagopal P, Murali R, Veeraraghavan VP, Sridevi G, Palanisamy CP, Jayaraman S. Effect of Seendhil polyherbal formulation in attenuating type-2 diabetes in STZ-induced experimental rats. International Journal of Drug Delivery Technology. 2026; 16(26s):981-989.
48. Manju NE, Natarajan A, Rebecca FS, Nivedha RP, Hemalatha R, Rajagopal P, Murali R, Veeraraghavan VP, Sridevi G, Palanisamy CP, Jayaraman S. Molecular mechanism to identify the effects of Seendhil polyherbal preparation on IRS-1/AKT/GLUT4/NRF2-KEAP-1 mediated signaling in SFZ-induced type-2 diabetic adult male rats. International Journal of Drug Delivery Technology. 2026;16(26s):972-980.
49. Palanisamy CP, Poompradub S, Sansanaphongpricha K, Jayaraman S, Subramani K, Sonsudin F. Biosynthesis of silver nanoparticles (AgNPs) using ethanolic extract of Nigella sativa (L.) seeds promotes wound healing via PDGF and VEGF signalling pathways activation. Biocatalysis and Agricultural Biotechnology. 2023; 54: 102970.